SAND 99-1015 J

Intracavity frequency doubling of a diode-pumped, external cavity, surface emitting semiconductor laser

T.D. Raymond, W.J. Alford, M.H. Crawford, A.A. Allerman

Sandia National Laboratories, Albuquerque, NM 87185-1423

Abstract

We present a compact, robust, solid-state blue light (490 nm) source capable of greater than 5 mW of output in a TEM_{00} mode. This device is an optically pumped, vertical external-cavity surface-emitting laser (VECSEL) with an intracavity frequency doubling crystal.

Compact, efficient blue sources are important for high- density optical storage devices, projection display lasers, and chemical sensing applications. A number of approaches using semiconductor lasers are being pursued for such sources including wide bandgap edge-emitting lasers[1], frequency-doubled edge emitting near infrared lasers[2], frequency-doubled lasers incorporating external build up cavities[3]. Except for the wide bandgap lasers, which are currently available at only a narrow band of near-UV/blue wavelengths, these approaches all suffer from complex optical configurations, complex electronics for wavelength stabilization, and the need for beam conditioning optics. Intracavity frequency doubling, while eliminating many of these undesirable requirements, has not been advantageous in edge emitting lasers because the intracavity power is not significantly larger than that available external[4] to the cavity. Vertical cavity surface-emitting lasers (VCSELs) provide good beam quality and high efficiency in the near infrared and red[5], and due to their low loss and small output coupling have high intracavity power. Despite these attributes, the short cavity length severely restricts the per-pass conversion doubling efficiency and has precluded the generation of frequency doubled powers in excess of a few nW[6] using these devices. The recent report of high power optically pumped vertical *external* cavity surface emitting lasers[7] (VECSELs) with cavities long enough to permit insertion of millimeter length doubling crystals suggests that intracavity frequency doubling could be efficient in that configuration. In this paper we report a diode-pumped VECSEL with an intracavity frequency doubling crystal to produce blue light around 490 nm.

Our device is depicted in Figure 1. It consists of a semiconductor gain region with an integrated high reflector, a frequency doubling crystal with an integrated curved high reflector, and a single-stripe diode pump laser with associated discrete focussing optics.

The semiconductor structure, shown in Figure 2, is grown via metal organic vapor phase epitaxy on a 0.65 mm thick GaAs wafer oriented 2° from the (100) towards the (110) plane. The high reflector is a distributed Bragg reflector (DBR) consisting of 27 quarter-wave stacks of alternating AlAs and GaAs layers. $Al_{0.08}Ga_{0.92}As$ layers absorb pump light, creating carriers that relax into the adjacent 8 nm thick compressively strained $In_{0.18}Ga_{0.82}As$ quantum wells to provide gain around 980 nm. The fifteen quantum wells, bounded on one side by 9 nm thick $GaAs_{0.80}P_{0.20}$

strain compensation layers and the other with the pump absorbing layers, are spaced to coincide with the anti-nodes of the standing electric field at the 980 nm design wavelength[7]. An InGaP cap layer mitigates carrier diffusion to the wafer surface and oxidation of the aluminum-bearing layers. No attempt was made to antireflection coat the upper surface of the wafer and consequently a short, low finesse cavity is formed between the DBR and the upper wafer surface. The InGaP/AlGaAs top structure was included to enable course tuning of this microcavity length by selective wet chemical etching, though no such tuning was employed here.

A 3 mm square piece of the nominally 0.65 mm thick semiconductor wafer is mounted onto a copper block attached to a miniature thermoelectric cooler. The copper block was maintained at less than 10°C for the data presented here, though the pumped region of the semiconductor is believed to have been many tens of degrees warmer. Course wavelength tuning is accomplished by changing the temperature of the copper block. This tuning is dominated by the temperature dependence of the quantum well gain and the thermally induced change in index of refraction of the semiconductor materials that shift the micro-cavity resonances. The gain region is pumped at Brewster's angle with 800 nm light from a 500 mW diode laser (SDL 2350-C). The 50 by 1 μm emitting region is oriented with the long dimension out of the plane of Fig. 1 to assist in projecting a circular pump spot with a ~100 μm e^{-2} diameter onto the wafer. Projection of a circular pump profile is accomplished with a 12 mm diameter, 25 mm radius of curvature mirror and a 2 mm thick fused silica plate oriented at Brewster's angle. A half wave plate rotates the pump polarization to minimize reflection losses on the wafer. While the pump laser is capable of 500 mW, the pump collection optics delivered only 330 mW to the wafer and of that, only 300 mW is absorbed.

The frequency doubling crystal is b-cut $KNbO_3$, 7.5 mm long, designed to Type I noncritically phase match 980 nm frequency doubling near room temperature. The acceptance bandwidth[8] of the crystal is approximately 2.8 cm^{-1} and its large angular acceptance of approximately 64 mrad permits cavity angular alignment with little effect on conversion efficiency. The intracavity crystal surface is planar and anti reflection coated (R<0.05%) for 980 nm; the other surface is polished to a 15 mm radius of curvature and is coated with a dielectric mirror highly reflective

(R>99.9%) at 980 nm but transmissive at 490 nm. When spaced 1-3 mm from the wafer, a stable cavity is formed with a TEM_{00} e^{-2} diameter slightly smaller than the projected pump spot. The theoretical per pass doubling efficiency[9] for this configuration is 1.6 %/Watt of circulating power under optimal phasematching conditions. For the results presented in this paper, the crystal was not temperature controlled.

The input/output power characteristic of this laser is shown in Figure 3. Laser threshold is approximately 110 mW of pump light. The intentionally low (0.029%) output coupling at 980 nm allows only about 1 mW of fundamental power to escape the cavity yet this implies a circulating power approaching 3.4 Watts. As expected, the output 490 nm power increases approximately quadratically with the circulating power to a pump-limited 5 mW. The data indicate a slight hysteretic effect believed to be thermal in origin. The blue output power was observed to have a noise spectral power less than 70 ppm/$Hz^{0.5}$ from 0 to 100 kHz; for comparison, the pump source and the 980 nm output had noise spectral powers less than the 9 ppm/$Hz^{0.5}$ noise floor of our detection system. Owing to the stable cavity and circular pump region, the laser output is TEM_{00} throughout the pump range. The inset in Fig. 3 illustrates that the beam profile which is radially symmetric, and approximately Gaussian with a near diffraction limited divergence of 10 mRad $1/e^2$ diameter, at maximum pump power. Measurements with a similar device pumped with a Ti:SAP laser indicate the formation of a thermally induced positive lens in the semiconductor. This thermally induced lens leads to a slight power dependence in the divergence of the output beam.

Even at the highest circulating power, the doubling efficiency is observed to be less than 0.15%/pass suggesting that the frequency doubling process is not well phasematched. The fundamental and frequency doubled laser spectra, plotted in Figure 4, support this conclusion. The high frequency modulation on both spectra is attributable to the well-resolved longitudinal modes of the laser. The center wavelength of 980 nm is significantly detuned from the phasematching wavelength of 982.7 nm and the lasing bandwidth of over 10 cm^{-1} FWHM (1 nm) is well in excess of the predicted[8] 2.8 cm^{-1} phasematching acceptance bandwidth. The modulation in the envelope of the 980 nm spectrum is due to an interference effect between the antireflection coated crystal face and the DBR. The modulation in the envelope of the 490 nm spectrum corresponds to the oscillations in the phasematching function[9]. Because the laser gain is highly homogeneous and the nonlinear loss is maximized for phasematched wavelengths, the laser tends not to operate near the phasematch wavelength where maximum conversion efficiency would be obtained. This is strikingly illustrated in Fig. 4 where, in spite of the relatively low power around 982.2 nm which produces it, the more favorable phasematching results in a relatively large peak in the doubled light near 491.1 nm. Attempts to tune the laser into phasematching simply by changing the temperature of the copper heat sink were unsuccessful.

In summary, we have shown that a diode-pumped VECSEL can be intracavity frequency doubled to produce light around 490 nm. Up to 5 mW of TEM_{00} blue-green light was generated with an optical-to-optical conversion efficiency of 1.5%. A significant improvement in the output blue power should be attained by more aggressive spectral control of the lasing wavelength and bandwidth.

The authors would like to thank Weng Chow and Arlee Smith for numerous discussions, Hong Hou for growing the first wafers, and Ronald Allman for his technical contributions. This work was conducted at Sandia National Laboratories which is a multi-program laboratory operated by Sandia Corporation, a Lockheed Martin Company, for the United States Department of Energy under Contract DE-AC04-94AL85000.

References

1. G. Fasol, S. Nakamura, and I. Davies, The Blue Laser Diode: GaN Based Light Emitters and Lasers, (Springer, New York, 1997).
2. L. Goldberg, L.E. Busse, and D. Mehuys, Appl. Phys. Lett. **63**, 2327 (1993); W.Wang, M.M. Fejer, R.H. Hammond, M.R. Beasley, and C.H. Ahn, Appl. Phys. Lett. **68**, 729 (1996).
3. W.J. Kozlovsky, W. Lenth, E.E. Latta, A. Moser, and G.L. Bona, Appl. Phys. Lett. **56**, 2291 (1990).
4. W.J. Kozlovsky, W.P. Risk, W. Lenth, B.G. Kim, G.L. Gona, H. Jaeckel, and D.J. Webb, Appl. Phys. Lett. **65**, 525 (1994).
5. W. W. Chow, K. D. Choquette, M. H. Crawford, K. L. Lear and G. R. Hadley, IEEE J. Quant. Elec. **33**, 1810 (1997).
6. N. Yamada, Y. Kaneko, S. Nakagawa, D.E. Mars, T. Takeuchi, and N. Mikoshiba, Appl. Phys. Lett. **68**, 1895 (1996).
7. M. Kuznetsov, F. Hakimi, R. Sprague and A. Mooradian, Photon. Tech. Lett. **9**, 1063 (1997).
8. G. Ghosh. Appl. Phys. Lett. **65**, p3311 (1995).
9. Calculated using SNLO, written by A.V.Smith. SNLO may be downloaded free of charge at www.sandia.gov/imrl/XWEB1128/xxtal.htm.

Figure Captions

Figure 1 The polarization of the diode pump laser (DL) is rotated with half wave plate ($\lambda/2$) before the beam is condensed with spherical mirror M1. The plate BP is used to condition the beam to project a circular profile on the semiconductor gain region (SGR). The SGR is mounted on a copper plate (Cu), thermoelectric cooler (TEC) and heat sink (HS). The curved mirror on the $KNbO_3$ crystal completes the VECSEL cavity.

Figure 2 The semiconductor gain region and the distributed Bragg reflector (DBR) are grown upon a GaAs substrate.

Figure 3 The output blue power (+) exceeds 5 mW for an incident pump power of approximately 300 mW. Although the output IR power (■) is only 1 mW, the circulating power in the cavity approaches 3.4 W. The inset shows the far-field intensity pattern for the blue beam.

Figure 4 The spectrum of the fundamental (a) and second harmonic (b) laser outputs. The crystal frequency-doubling phasematch peak is located near 982.7nm.

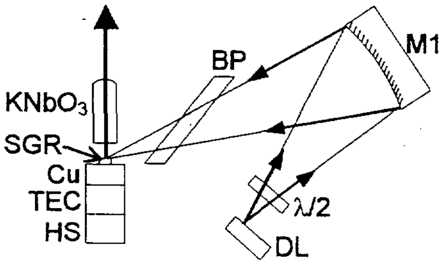

Figure 1

40 nm	$In_{0.49}Ga_{0.51}P$	
100 nm	$Al_{0.30}Ga_{0.70}As$	
40 nm	$In_{0.49}Ga_{0.51}P$	
100 nm	$Al_{0.30}Ga_{0.70}As$	
48 nm	$In_{0.49}Ga_{0.51}P$	
303 nm	$Al_{0.50}Ga_{0.50}As$	
30 nm	$Al_{0.08}Ga_{0.92}As$	
106 nm	$Al_{0.08}Ga_{0.92}As$	
8 nm	$In_{0.18}Ga_{0.82}As$	
9 nm	$GaAs_{0.80}P_{0..20}$	
116 nm	$Al_{0.08}Ga_{0.92}As$	
[redacted]	[redacted]	[redacted]
219 nm	$Al_{0.30}Ga_{0.70}As$	
68 nm	GaAs	
Substrate	GaAs (100)2°>(110)	

Figure 2

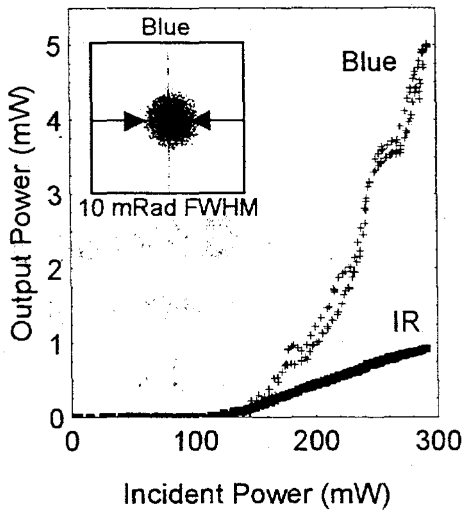
Blue
10 mRad FWHM
Blue
IR
Output Power (mW)
0
1
2
3
4
5
0
100
200
300
Incident Power (mW)

Figure 3

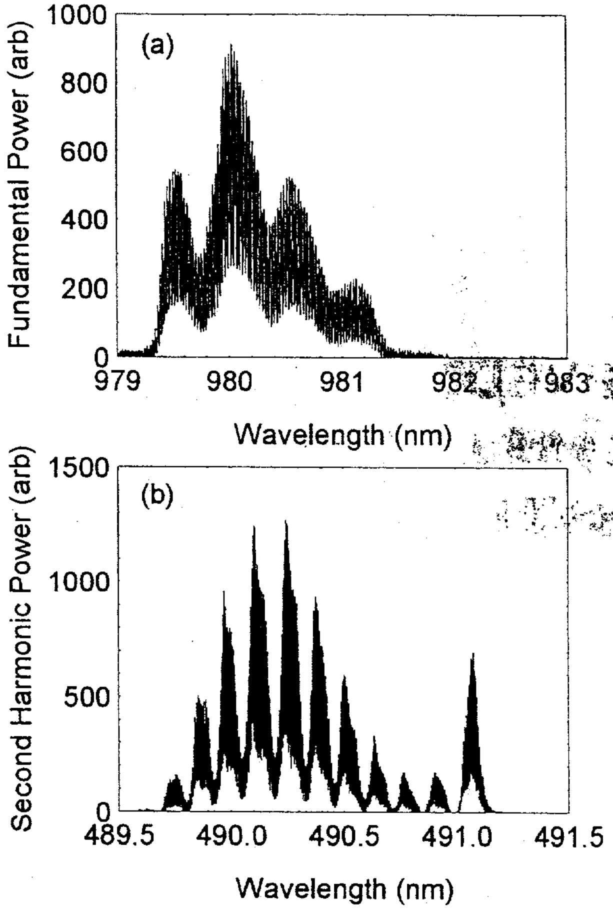
(a)
Fundamental Power (arb)
1000
800
600
400
200
0
979
980
981
982
983
Wavelength (nm)
(b)
Second Harmonic Power (arb)
1500
1000
500
0
489.5
490.0
490.5
491.0
491.5
Wavelength (nm)

Figure 4